Cell, Volume *134*

Supplemental Data

Acetylated Lysine 56 on Histone H3 Drives Chromatin Assembly after Repair and Signals for the Completion of Repair

Chin-Chuan Chen, Joshua J. Carson, Jason Feser, Beth Tamburini, Susan Zabaronick, Jeffrey Linger, and Jessica K. Tyler

Supplementary Material

Table 1. Genotypes of yeast strains used in these studies.

Name	Genotype
JKT010	*MAT a; his3-11; leu2-3,112; lys2; trp1-1; ura3-1; bar1::LEU2 (Adkins et al., 2004)*
JKT018	*MAT a; his3-11; leu2-3,112; lys2; trp1-1; ura3-1; bar1::LEU2; asf1::his5+ (Adkins et al., 2004)*
JKT200	MAT α ho hml::ADE1 mata::hisG hmr::ADE1 leu2(Asp-718-SalI)-URA3-pBR322-HOcs ade3::GAL::HO ade1 lys5 ura3-52 asf1::kan *This study*
JCY001	MATα ho hml::ADE1 mata::hisG hmr::ADE1 his4::-URA3-leu2-(Xho1 to Asp718)-his4 leu2::HOcs ade3::GAL::HO ade1 lys5 ura3-52 asf1::kan *This study*
JCY005	MATα ho hml::ADE1 mata::hisG hmr::ADE1 leu2(Asp-718-SalI)-URA3-pBR322-HOcs ade3::GAL::HO ade1 lys5 ura3-52 sml1::HPH *This study*
JCY006	MATα hml::ADE1 HO::ADE1 hmr::ADE1 ade1 leu2-3,112 lys5 ura3-52 ade3::Gal10:HO ku::Kan *This study*
JCY010	MATα ho hml::ADE1 mata::hisG hmr::ADE1 leu2(Asp-718-SalI)-URA3-pBR322-HOcs ade3::GAL::HO ade1 lys5 ura3-52 sml1::HPH asf1::kan *This study*
JCY014	MATa his3-11 leu2-3,112 lys2 trp1-1 ura3-1 bar1::LEU2 sml1::HPH rad53::kan asf1::his *This study*
JCY017	MATα ho hml::ADE1 mata::hisG hmr::ADE1 leu2(Asp-718-SalI)-URA3-pBR322-HOcs ade3::GAL::HO ade1 lys5 ura3-52 sml1::HPH mec1::His *This study*
JRY001	MATa his3-11 leu2-3,112 lys2 trp1-1 ura3-1 bar1::LEU2 sml1::HPH (Ramey et al., 2004)
JRY002	MATa his3-11 leu2-3,112 lys2 trp1-1 ura3-1 bar1::LEU2 sml1::HPH asf1::his5+ (Ramey et al., 2004)
JRY003	MATa his3-11 leu2-3,112 lys2 trp1-1 ura3-1 bar1::LEU2 sml1::HPH rad53::kan (Ramey et al., 2004)
JRY017	MATα hml::ADE1 HO::ADE1 hmr::ADE1 ade1 leu2-3,112 lys5 ura3-52 ade3::Gal10:HO asf1::Kan *This study*
JFY001	MATα ho hml::ADE1 mata::hisG hmr::ADE1 leu2(Asp-718-SalI)-URA3-pBR322-HOcs ade3::GAL::HO ade1 lys5 ura3-52 sml1::HPH mec1::His asf1::kan *This study*
YMV002	MATα ho hml::ADE1 mata::hisG hmr::ADE1 his4::-URA3-leu2-(Xho1 to Asp718)-his4 leu2::HOcs ade3::GAL::HO ade1 lys5 ura3-52 (Vaze

	et al., 2002)
YMV002-1	MATα ho hml::ADE1 mata::hisG hmr::ADE1 his4::-URA3-leu2-(Xho1 to Asp718)-his4 leu2::HOcs ade3::GAL::HO ade1 lys5 ura3-52 yku70::Kan (Vaze et al., 2002)
YMV045	MATα ho hml::ADE1 mata::hisG hmr::ADE1 leu2(Asp-718-SalI)-URA3-pBR322-HOcs ade3::GAL::HO ade1 lys5 ura3-52 (Vaze et al., 2002)
YMV046	MATα ho hml::ADE1 mata::hisG hmr::ADE1 leu2(Asp-718-SalI)-URA3-pBR322-HOcs ade3::GAL::HO ade1 lys5 ura3-52 rad52::HPH (Vaze et al., 2002)
YMV057	MATα ho hml::ADE1 mata::hisG hmr::ADE1 his4::-URA3-leu2-(Xho1 to Asp718)-his4 leu2::HOcs ade3::GAL::HO ade1 lys5 ura3-52 srs2::HPH (Vaze et al., 2002)
JKM179	MAT =alpha ΔHO::Ade1 Δhml::ADE1 Δhmr::Ade1 ade1 leu2-3,112 lys5 ura3-52 ade3::Gal 10:HO (Lee et al., 1998)
YTT035	MATα ΔHO::Ade1 Δhml::ADE1 Δhmr::Ade1 ade1 leu2-3,112 lys5 ura3-52 ade3::Gal 10:HO FlagHHT1::LEU (Tsukuda et al., 2005)
BAT009	MATa ade2-1 can1-100 his3-11 leu2-3,112trp1-1 ura3-1 GAL pGAL-HO::ADE3 (Tamburini and Tyler, 2005)
BAT058	MATα ΔHO::Ade1 Δhml::ADE1 Δhmr::Ade1 ade1 leu2-3,112 lys5 ura3-52 ade3::Gal 10:HO FlagHHT1::LEU arp8::KAN *This study*
BAT061	MATα ΔHO::Ade1 Δhml::ADE1 Δhmr::Ade1 ade1 leu2-3,112 lys5 ura3-52 ade3::Gal 10:HO FlagHHT1::LEU mre11::KAN *This study*
BAT062	MATα ΔHO::Ade1 Δhml::ADE1 Δhmr::Ade1 ade1 leu2-3,112 lys5 ura3-52 ade3::Gal 10:HO FlagHHT1::LEU asf1::HYGRO *This study*
CCY015	MATα ho hml::ADE1 mata::hisG hmr::ADE1 leu2(Asp-718-SalI)-URA3-pBR322-HOcs ade3::GAL::HO ade1 lys5 ura3-52 sml1::HPH tel1::TRP *This study*
CCY017	MATα ho hml::ADE1 mata::hisG hmr::ADE1 leu2(Asp-718-SalI)-URA3-pBR322-HOcs ade3::GAL::HO ade1 lys5 ura3-52 sml1::HPH tel1::TRP mec1::His *This study*
JLY075	MATa ade2-1 can1-100 his3-11 leu2-3,112 trp1-1 ura3-1 GAL pGAL-HO::ADE3 rad52::KAN *This study*
BAT063	MATa ade2-1 can1-100 his3-11 leu2-3,112 trp1-1 ura3-1 GAL pGAL-HO::ADE3 asf1::HYGRO *This study*
JFY014	MATa ade2-1 can1-100 his3-11 leu2-3,112 trp1-1 ura3-1 GAL pGAL-HO::ADE3 rtt109::kan *This study*
JFY017	MATα ho hml::ADE1 mata::hisG hmr::ADE1 leu2(Asp-718-SalI)-URA3-pBR322-HOcs ade3::GAL::HO ade1 lys5 ura3-52 asf1::kan Ddc2-13Myc::TRP1 *This study*
JFY016	MATα ho hml::ADE1 mata::hisG hmr::ADE1 leu2(Asp-718-SalI)-URA3-pBR322-HOcs ade3::GAL::HO ade1 lys5 ura3-52 Ddc2-13Myc::TRP1 *This study*
JFY013	ho hmlΔ::ADE1 mataΔ::hisG hmrΔ::ade1 leu2::leu2(Asp-718-SalI)-

	URA3-pBR322-HOcs ade3::GAL::HO ade1 lys5 ura3-52 trp1 (trp1::hisG?) rtt109::kan *This study*
MSY421	MATa Δ(hht1-hhf1) Δ(hht2-hhf2) leu2-3,112 ura3-62 trp1 his3 p(TRP1,CEN,hht2-HHF2) (Recht et al., 2006)
MSY421 K56Q	MATa Δ(hht1-hhf1) Δ(hht2-hhf2) leu2-3,112 ura3-62 trp1 his3 p(TRP1,CEN,hht2-HHF2) hht2 K56Q (Recht et al., 2006)
MSY421 K56R	MATa Δ(hht1-hhf1) Δ(hht2-hhf2) leu2-3,112 ura3-62 trp1 his3 p(TRP1,CEN,hht2-HHF2) hht2 K56R (Recht et al., 2006)
MSY421 K56Q asf1Δ	MATa Δ(hht1-hhf1) Δ(hht2-hhf2) leu2-3,112 ura3-62 trp1 his3 p(TRP1,CEN,hht2-HHF2) hht2 K56Q asf1::KAN (Recht et al., 2006)
MSY421 K56R asf1Δ	MATa Δ(hht1-hhf1) Δ(hht2-hhf2) leu2-3,112 ura3-62 trp1 his3 p(TRP1,CEN,hht2-HHF2) hht2 K56R asf1::KAN (Recht et al., 2006)
MSY421 asf1Δ	MATa Δ(hht1-hhf1) Δ(hht2-hhf2) leu2-3,112 ura3-62 trp1 his3 p(TRP1,CEN,hht2-HHF2) asf1::KAN (Recht et al., 2006)

Supplementary Methods:

Chromatin disassembly and reassembly analysis

Three separate isolates of each strain were grown up overnight in YPD. Cultures were diluted down to OD of ~.3 in YEP-R and allowed to grow back for at least 4hrs until the cells reached an optical density of approximately OD_{600} 0.5. Samples were taken for ChIP analyses and to make genomic DNA (for the DNA damage and repair analyses described below) at the time points indicated in the Figures; the 0hr samples were taken for DNA and ChIP (1.25×10^8 cells) analysis prior to addition of galactose to 2%, followed by taking samples for ChIP and Genomic preps at the indicated time points after adding galactose. Addition of galactose induces the HO endonuclease which is under the control of the GAL1 promoter. While galactose is present, numerous rounds of repair and re-cutting of the HO site occur, each time resulting in switching of the mating type. After the 2hr time point samples were taken, glucose was added to 2% to repress the HO endonuclease. ChIP analyses were performed as previously described (Tamburini and Tyler, 2005), using 2.5μl of antisera to H3 (Abcam #1791) or 4μl of antisera to FLAG (Sigma #F3165).

Real-time PCR was used to quantitate amounts of DNA fragments in the immunoprecipitated (IP) and input samples from the ChIP analyses, using the ABI 7700 sequence detector and Taqman PCR Master Mix protocol (ABI). Each PCR reaction was performed in triplicate with cycling conditions as follows: 50° for 2min, 95° for 10 min then 40 cycles of 95° for 15 s and 60° for 1 min. The primers used were designed using the ABI Primer Express software (ABI) and the sequences are available upon request. Each PCR

was carried out in triplicate and was multiplexed with a primer set specific to either 0.6kb or 2kb from the HO lesion, and a primer set to the internal control *SMC2* gene (Martin et al., 1999) using FAM and VIC probes designed using the ABI Primer Express software (Applied Biosystems). The threshold, or CT value, was set so that the fluorescence signal was above the baseline noise, and as low as possible in the exponential amplification phase. Fold change over the *SMC2* control was calculated for each input using the following equation: (log (base 2) SMC2 primer pair CT from input (1:5000) - HO primer pair CT from input (1:5000)). Fold change over the *SMC2* control was calculated for each IP using the following equation: (log (base 2) SMC2 primer pair CT from IP (1:100) - HO primer pair CT from IP (1:100)). The ratio of the IP to the input was calculated as the relative fold change over input using the following equation: (log (base 2) SMC2 primer pair CT from IP (1:100) - HO primer pair CT from IP (1:100))/ (log (base 2) SMC2 primer pair CT from input (1:5000) - HO primer pair CT from input (1:5000)). A change in CT value of one unit was determined empirically for each primer pair to be very close to two indicating, approximately, a two fold change in amplification per cycle over the range of template amounts used in these analyses. The concentration of primers, probes, and template DNA that yielded the optimal amplification in the linear range in real time was empirically determined. P-values were determined using the unpaired Students T-test using Prism software (GraphPad Software, Inc). Plotted are the average and standard error of the mean of three independent cultures for each experiment.

Primer pairs / probe sequences for ChIP analysis of HO site at MAT:

SMC2 primer pair: F-GGTCCGGTAAGTCGAACATTTT R-CTCGCACAGTGCTCATTGATG

SMC2 Probe sequence: 6FAM ACGCCATTTGCTTCGTGCTCGGTA TAMRA

0.6kb HO primer pair: F-TTGGATCTTAACAAACCGTAAAGGT R-GGTAACTAGCAAACAAAGGAAAGTCA

0.6kb HO Probe sequence: VIC TCATCGAGCCCGTGAAGCATTCG TAMRA

2.0kb HO primer pair: F-CCATCGTGTTCATGGATCCTT R-AGAACATCCAGATTTGAACCGAA

2.0kb HO Probe sequence: VIC ACTGCCCATGCGGTTCACATGACTT TAMRA

DNA damage and repair quantitation of the HO site at *MAT*

Cutting, repair and mating type switching of the HO lesion at *MAT* was measured by PCR amplification of genomic DNA templates taken from the time courses described above, using primers flanking the HO site in the *MAT* locus, as described previously (Ramey et al., 2004). The cleaved HO site at *MAT* is repaired by copying the alpha sequences from HML or the a sequences from HMR, depending on the original mating type of the yeast. Due to the size difference between the a sequences and alpha sequences that are copied into the *MAT* locus during repair of the HO lesion, the use of a PCR primer pair that amplifies across the HO sequence allows determination of whether the sequences at *MAT* are a or alpha (i.e. *MAT*a or *MAT*alpha). As such, this allows us to follow the repair event and mating type switching by PCR analysis. *MAT*a yields a 1.0kb PCR product, *MAT* alpha yields a 1.1kb PCR product, while cut DNA yields no *MAT* PCR product. At time 0, the total amount of *MAT*a PCR product plus *MAT* alpha PCR product is normalized to 100%. Primers to the *RAD27* gene were included in the multiplex PCR as an internal control. The number of PCR cycles to produce amplification in the linear range was determined empirically. PCR Products were resolved on a 2% agarose gel, and stained with ethidium bromide. The ratio of the *MAT* product to the *RAD27* control product was quantified using Labworks (GelPro4.0, Media Cybernetics, LP). As described above, galactose was added at time 0 to induce the HO endonuclease and

glucose was added after 2 hours to repress the HO endonuclease. During the 2 hours in glucose numerous rounds of cutting and repair, and hence mating type switching occur, explaining why the population switches to a mixture of *MAT* a or *MAT* alpha after repression of the HO endonuclease by glucose.

Primer pairs for cutting and repair quantitation at *MAT*:

MAT primer pair: F-AGGTAAATTACAGCAAATAG R-AACAACAACCTAGAGTAATG

RAD27 primer pair: F-ACATCGCGCAAATGAAGGTT R-TCAATTCCCAGAAAAACTG

Analysis of SSA repair and Rad53 activation

The strains for the SSA repair analysis carried an uncleavable region of homology to the HO site either 5kb or 30kb proximal (depending on the strain used) to the cleavable HO site, on the same chromosome (Vaze et al., 2002). Upon induction of the HO break, extensive resection occurs until the homologous uncleaveable HO site becomes single stranded, at which the point the two homologous single stranded HO sequences anneal and the resulting single stranded overhangs are trimmed off. The product of the repair reaction therefore has a deletion of the region between the HO sites, and now only bears an uncleavable HO sequence, preventing further cutting of the HO site during growth on galactose. As such, there is only one round of cutting and repair during these analyses. PCR analysis was used to follow these events as described below. Cultures were diluted down to OD_{600} of ~.3 in YEP-R and allowed to grow back for at least 4hrs until the cells reached an optical density of approximately OD_{600} 0.5. Samples were taken for Rad53 western blots, to make genomic

DNA (for the DNA damage and repair analysis) or for ChIP at the time points indicated in the Figures; the 0hr samples were taken prior to addition of galactose to 2%. Cutting and repair of the HO site in the single strand annealing strains was performed using the three primers indicated in Fig. 3B. PCR analysis prior to repair yields a 1.7kb PCR product, during DNA damage yields no PCR product, and following repair by SSA yields a 3.0kb product. Primers to the *RAD3* gene were included in the multiplex PCR as an internal control. The number of PCR cycles to produce amplification in the linear range was determined empirically.

Protein samples were prepared by TCA precipitation as previously described (Keogh et al., 2006). Samples were resolved on 8% SDS PAGE gels and Rad53 was detected by western blotting using an antibody against Rad53 at 1:200 dilution (from Santa Cruz, sc-6749) or one that was generously provided by John Diffley.

Primer pairs for analysis of SSA cutting and repair:

Control primer pair:

RAD3A---GAT AAG ATT GCG ACA AAA GAG GAT A

RAD3D---GTG GGA CGA GAC GTT TAG ATA GTA A

HO flanking primer set:

SSA1---CCG CTG AAC ATA CCA CGT TG

SSA2---CAC TTC CAG ATG AGG CGC TG

SSA3---TGA ACT CTG GTG TCT TTT AG

Chromatin immunoprecipitation of phosphorylated H2A and Ddc2

Samples were taken at the time points indicated in the figures during SSA for ChIP analysis, and were processed as previously described (Adkins et al., 2004) using 1 µl antisera to

phosphoH2A (kindly provided by William Bonner) or 4 µl of antisera to Myc (Santa Cruz). A region proximal to the HO lesion was amplified, and primers to a region in the telomere on the right arm of chromosome six were included in the multiplex PCR reactions as an internal control. The number of PCR cycles to produce amplification in the linear range was determined empirically.

Primer pairs for ChIP analysis of HO site during SSA:

For the HO Cut Site:

5': CCAAATCTGATGGAAGAATGGG

3': CCGCTGAACATACCACGTTG

For the control on telemere VI Right Arm:

5': GGATTTTACCAACGACTTCGTCTCA

3': CGCTATTCCAGAAAGTAGTCCAGC

HO endonuclease and drug sensitivity plate assays

Yeast strains were grown overnight in rich media + 2% raffinose. Cells were diluted and grown to OD_{600} of ~0.75 and concentrated to an OD_{600} of 1.0 or higher to plate in 10-fold serial dilutions onto YPD, rich media + 2% raffinose + 2% galactose, or the indicated amount of MMS or zeocin.

Cell Death Assays

Logarithmically growing cultures were assayed for cell death and cell cycle stage of dead cells. For viability staining (Molecular Probes; LIVE/DEAD® Yeast Viability Kit) the manufacturers protocol was followed exactly. FUN1 was used at a 1:1000 dilution and Calcofluor White M2R was used at a 1:2000 dilution. Fields of cells were scored as either alive or dead. Visualization was performed with an Eclipse E800 fluorescence microscope (Nikon), equipped with a CoolSnap HQ camera (Photometrics), and Meta-Morph analysis software. Samples of the same cultures were assayed in this manner prior to addition of 2ug/ml Zeocin (O time) and 9 or 24 hours after addition of Zeocin.

Supplemental Figures

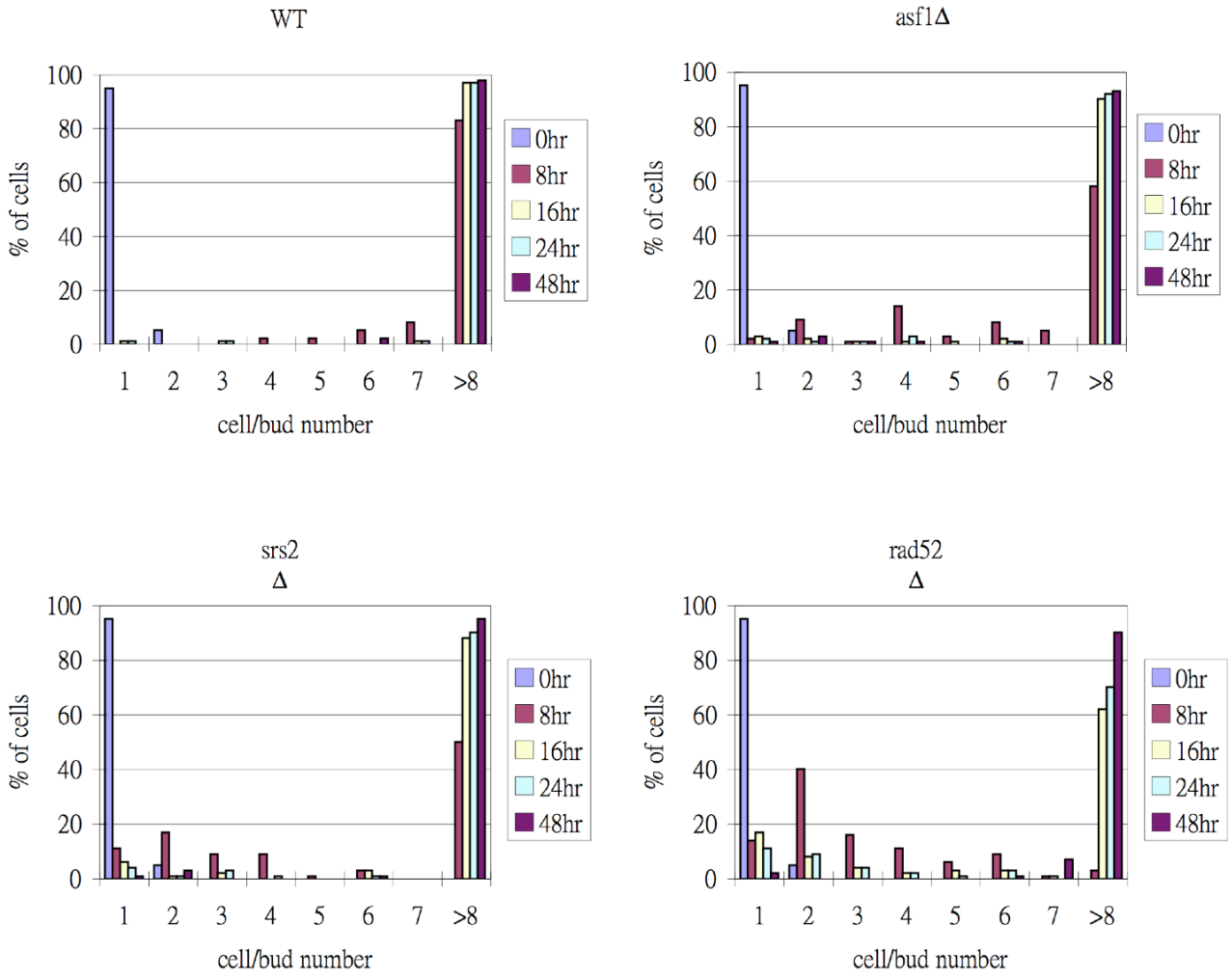

Supplemental Figure 1. The recovery defect seen in the asf1Δ mutant upon induction of the HO break is not a mere consequence of a slow growth defect of the strain. The analysis was performed with the identical strains used in Fig. 4B, but with plating onto glucose instead of galactose.

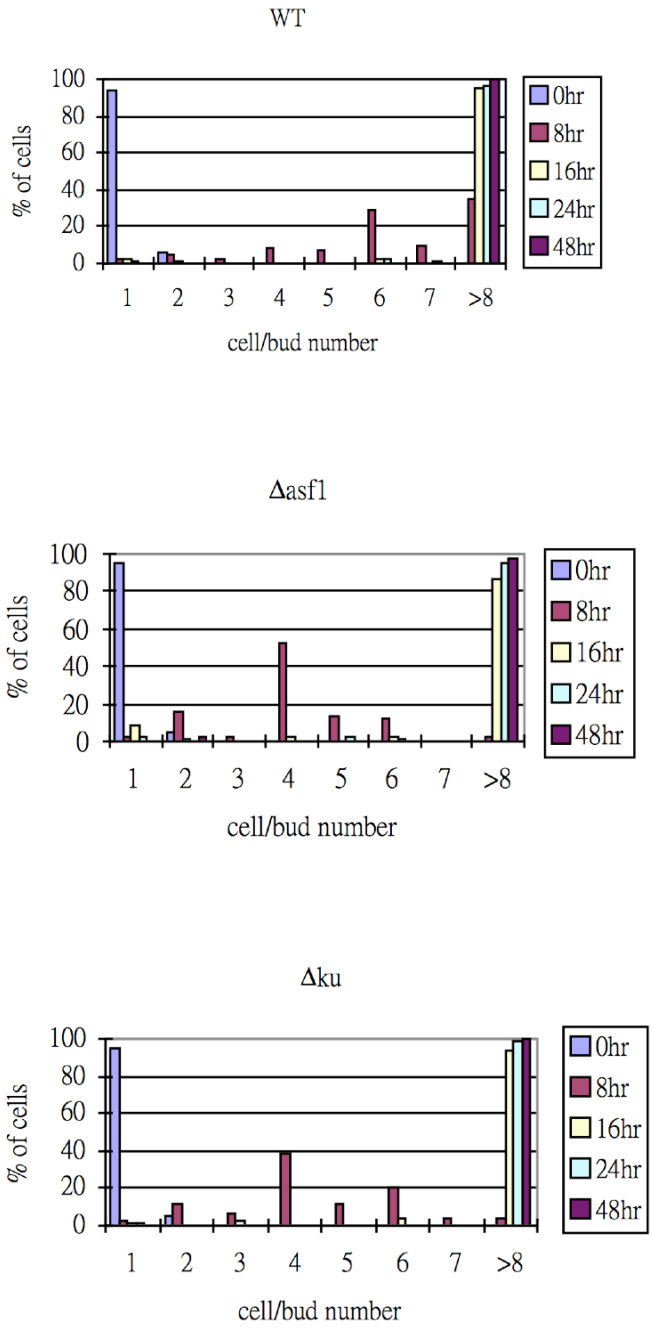

Supplemental Figure 2. The adaptation defect seen in the asf1Δ mutant upon induction of the HO break is not a mere consequence of a slow growth defect of the strain. The analysis was performed with the identical strains used in Fig. 5C, but with plating onto glucose instead of galactose.

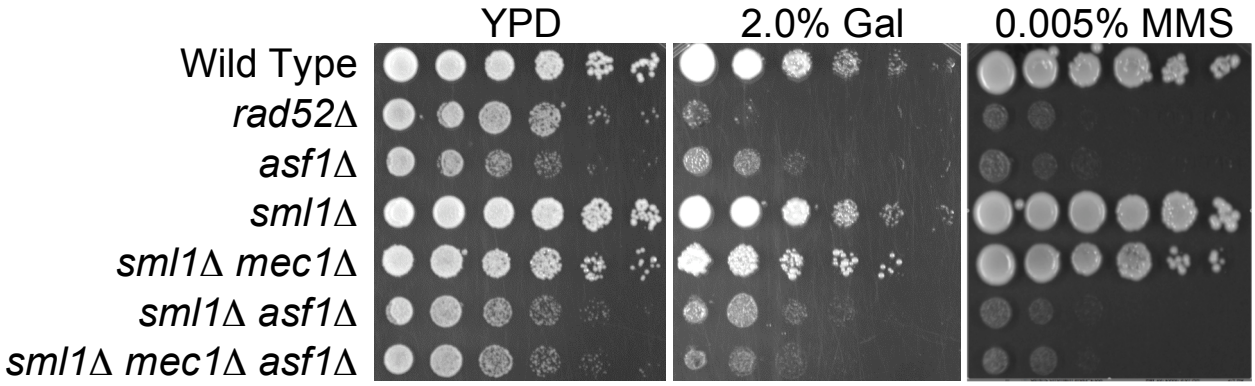

Supplemental Figure 3. Inactivation of MEC1 does not fix the DNA damage sensitivity of the asf1 mutant. 10-fold serial dilution analysis of the indicated 5kb resection SSA yeast strains WT (YMV045), *rad52*Δ (YMV046), *asf1*Δ (JKT200), *sml1*Δ (JCY005), *sml1*Δ*mec1*Δ (JCY017), *sml1*Δ*asf1*Δ (JCY010), and *sm1*Δ*mec1*Δ*asf1*Δ (JFY001) to a single HO lesion (induced by galactose) and MMS. Albeit, it is still possible that additional checkpoint components, such as Tel1 may be maintaining checkpoint arrest in the absence of MEC1.

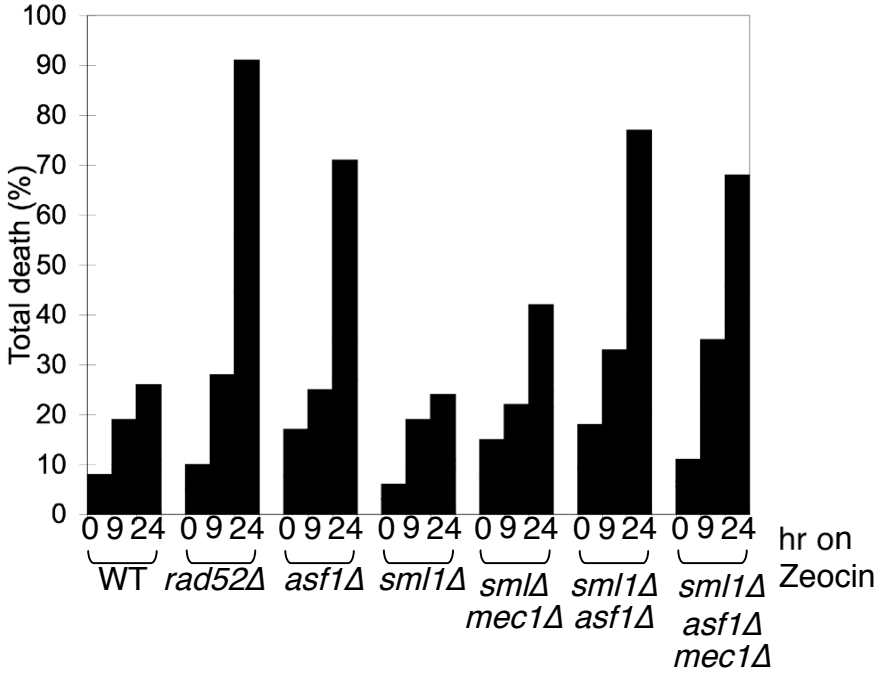

Supplemental Figure 4. The asf1 mutants die upon exposure to DNA damage, and the death is not rescued by deletion of MEC1. Quantitation of proportion of cell death determined using the live/dead analysis, in the same yeast strains used in Suppl. Fig. 3, following 0, 9 or 24 hours of exposure to zeocin.

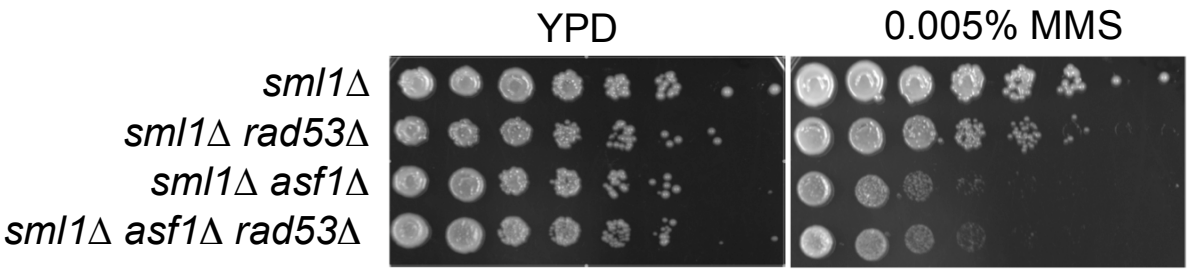

Supplemental Figure 5. Inactivation of RAD53 does not rescue the DNA damage sensitivity of the asf1 mutant. 10-fold serial dilution analysis of the indicated strains, *sml1*Δ (JRY001), *sml1*Δ*rad53*Δ (JRY003), *sml1*Δ*asf1*Δ (JRY002) and *sml1*Δ*asf1*Δ*rad53*Δ (JCY014) to show sensitivity to MMS. It is still possible that additional checkpoint components, such as Chk1 may be maintaining the checkpoint arrest in the absence of Rad53, as suggested below.

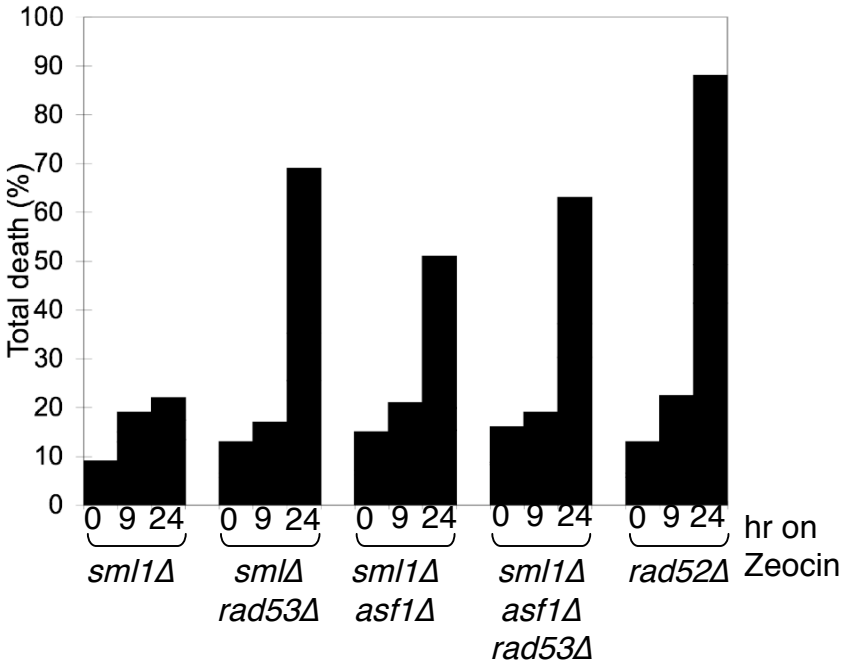

Supplemental Figure 6. Deletion of RAD53 does not rescue the cell death of asf1 mutants upon exposure to DNA damaging agents. Quantitation of proportion of cell death in the same yeast strains used in Suppl. Fig. 5, plus a *rad52*Δ strain (YMV046), following 0, 9 or 24 hours of exposure to zeocin.

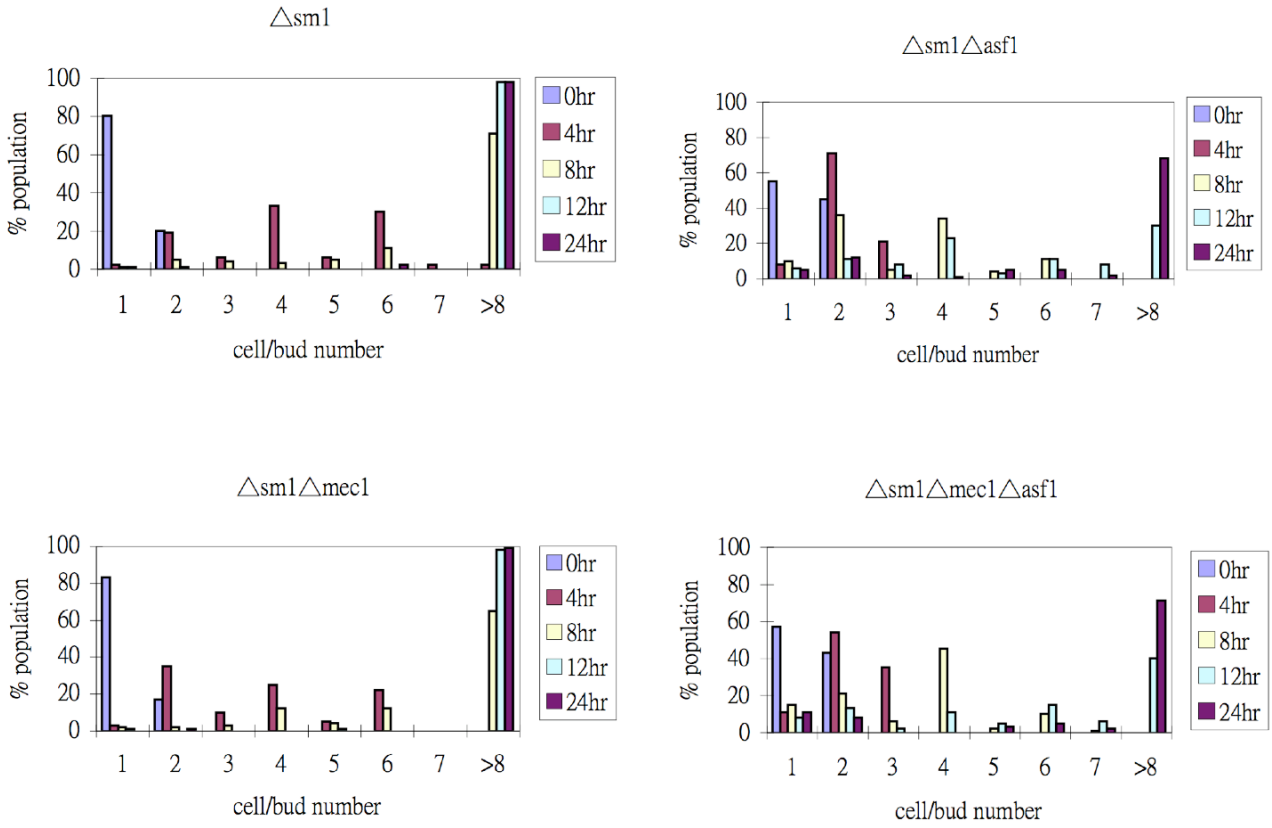

Supplemental Figure 7. Deletion of MEC1 does not rescue the DNA damage checkpoint recovery defect of the asf1 mutant. Colony formation analysis of the indicated 5kb resection SSA yeast strains *sml1*Δ (JCY005), *sml1*Δ*mec1*Δ (JCY017), *sml1*Δ*asf1*Δ (JCY010), and *sm1*Δ*mec1*Δ*asf1*Δ (JFY001) following induction of a single HO lesion (induced by galactose), as in Fig. 4. This result indicates that checkpoint arrest is maintained in the absence of MEC1 in the asf1 mutants, suggesting that other checkpoint kinases may also be activated.

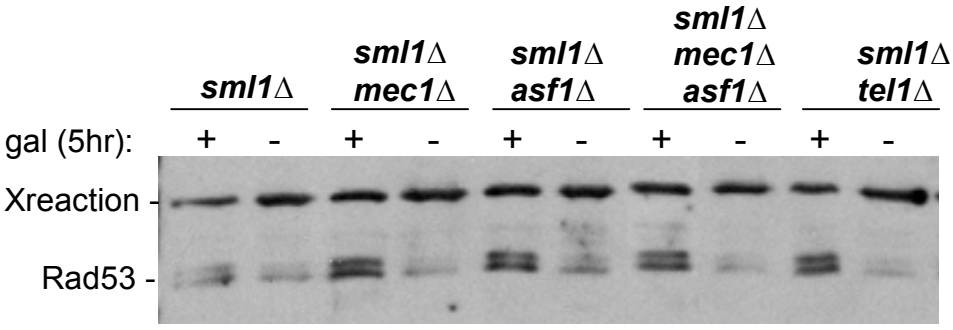

Supplemental Figure 8. Persistent Rad53 activation upon deletion of MEC1 in the asf1 mutant. Western blot analysis of the indicated 5kb resection SSA yeast strains *sml1*Δ (JCY005), *sml1*Δ*mec1*Δ (JCY017), *sml1*Δ*asf1*Δ (JCY010), *sm1*Δ*mec1*Δ*asf1*Δ (JFY001) and *sml1*Δ*tel1*Δ (CCY005) following induction of a single HO lesion by treatment with galactose for 5 hours "+", or in the absence of galactose "-". "Xreaction" refers to a crossreacting band that serves as a normalization control for loading. Phosphorylation of rad53 is seen in the absence of MEC1 upon induction of the HO break, suggesting that Rad53 is phosphorylated by another checkpoint kinase in the absence of Asf1 and Mec1. The persistent phosphorylation of Rad53 even in the strains that have Asf1 may reflect a requirement for the DNA damage checkpoint proteins to promote proper DNA repair, although this has not been investigated.

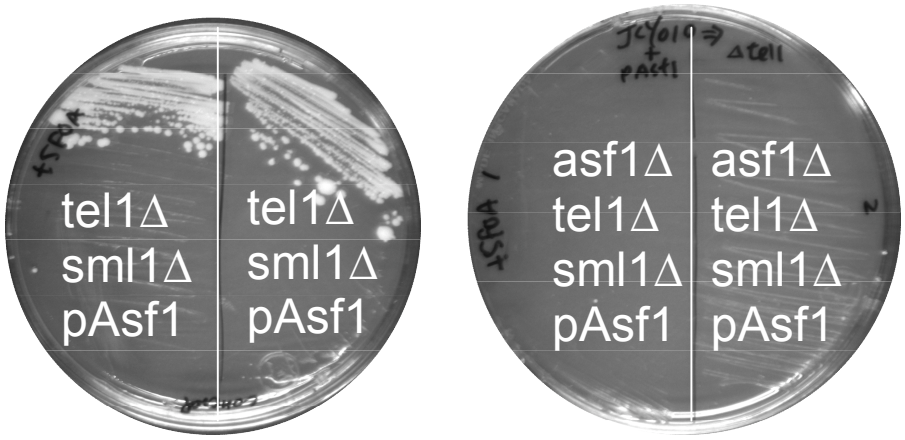

Supplemental Figure 9. Synthetic lethality upon deletion of both ASF1 and TEL1. The URA3 based plasmid pAsf1 was introduced into the sml1Δasf1Δ strain JCY010, followed by deletion of TEL1, to make strain sml1Δasf1Δtel1ΔpAsf1. The requirement for pAsf1 for viability was determined by plating this strain onto 5’FOA to kill cells carrying the pAsf1 plasmid. As a control, the URA3 based plasmid pAsf1 was introduced into the tel1Δsml1Δ strain CCY015 to make strain sml1Δasf1ΔpAsf1.

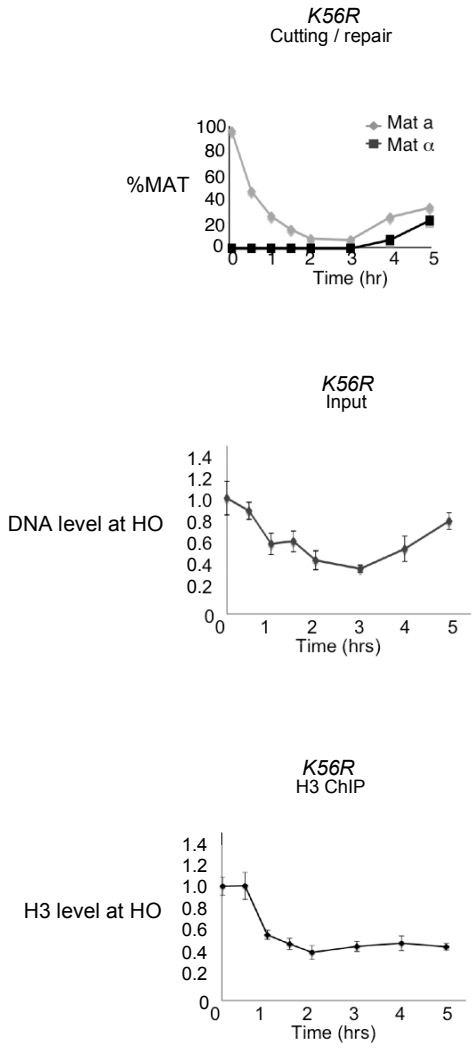

Supplemental Figure 10. Substitution of histone H3 lysine 56 to an arginine prevents chromatin reassembly after DNA repair. The top panel shows the quantitation of the cutting and repair analysis of the HO site at MAT in a strain carrying the H3 K56R mutation. The middle panel shows the input to the histone H3 ChIP analysis from the same time course as above. The lower panel shows the H3 ChIP analysis from the same time course as above.

Supplemental References

Adkins, M. W., Howar, S. R., and Tyler, J. K. (2004). Chromatin disassembly mediated by the histone chaperone Asf1 is essential for transcriptional activation of the yeast PHO5 and PHO8 genes. Mol Cell *14*, 657-666.

Keogh, M. C., Mennella, T. A., Sawa, C., Berthelet, S., Krogan, N. J., Wolek, A., Podolny, V., Carpenter, L. R., Greenblatt, J. F., Baetz, K., and Buratowski, S. (2006). The Saccharomyces cerevisiae histone H2A variant Htz1 is acetylated by NuA4. Genes Dev *20*, 660-665.

Lee, S. E., Moore, J. K., Holmes, A., Umezu, K., Kolodner, R. D., and Haber, J. E. (1998). Saccharomyces Ku70, mre11/rad50 and RPA proteins regulate adaptation to G2/M arrest after DNA damage. Cell *94*, 399-409.

Martin, S. G., Laroche, T., Suka, N., Grunstein, M., and Gasser, S. M. (1999). Relocalization of telomeric Ku and SIR proteins in response to DNA strand breaks in yeast. Cell *97*, 621-633.

Ramey, C. J., Howar, S., Adkins, M., Linger, J., Spicer, J., and Tyler, J. K. (2004). Activation of the DNA damage checkpoint in yeast lacking the histone chaperone anti-silencing function 1. Mol Cell Biol *24*, 10313-10327.

Recht, J., Tsubota, T., Tanny, J. C., Diaz, R. L., Berger, J. M., Zhang, X., Garcia, B. A., Shabanowitz, J., Burlingame, A. L., Hunt, D. F.*, et al.* (2006). Histone chaperone Asf1 is required for histone H3 lysine 56 acetylation, a modification associated with S phase in mitosis and meiosis. Proc Natl Acad Sci U S A *103*, 6988-6993.

Tamburini, B. A., and Tyler, J. K. (2005). Localized histone acetylation and deacetylation triggered by the homologous recombination pathway of double-strand DNA repair. Mol Cell Biol *25*, 4903-4913.

Tsukuda, T., Fleming, A. B., Nickoloff, J. A., and Osley, M. A. (2005). Chromatin remodelling at a DNA double-strand break site in Saccharomyces cerevisiae. Nature *438*, 379-383.

Vaze, M. B., Pellicioli, A., Lee, S. E., Ira, G., Liberi, G., Arbel-Eden, A., Foiani, M., and Haber, J. E. (2002). Recovery from checkpoint-mediated arrest after repair of a double-strand break requires Srs2 helicase. Mol Cell *10*, 373-385.